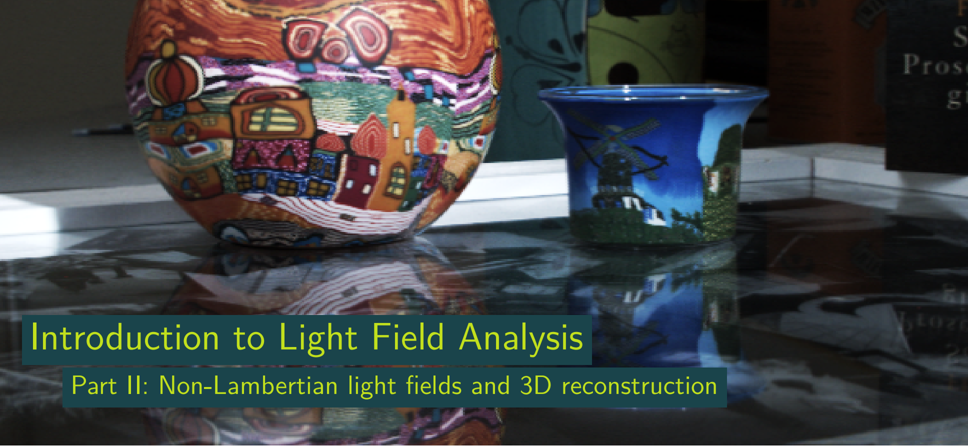

Introduction to Light Field Analysis

Part II: Non-Lambertian light fields and 3D reconstruction

Bastian Goldlücke

Training School on Plenoptic Sensing
15.3.2017

CVIA computer vision and image analysis

Universität Konstanz

What do these images tell you about the scene?

The light field: densely sampled view points

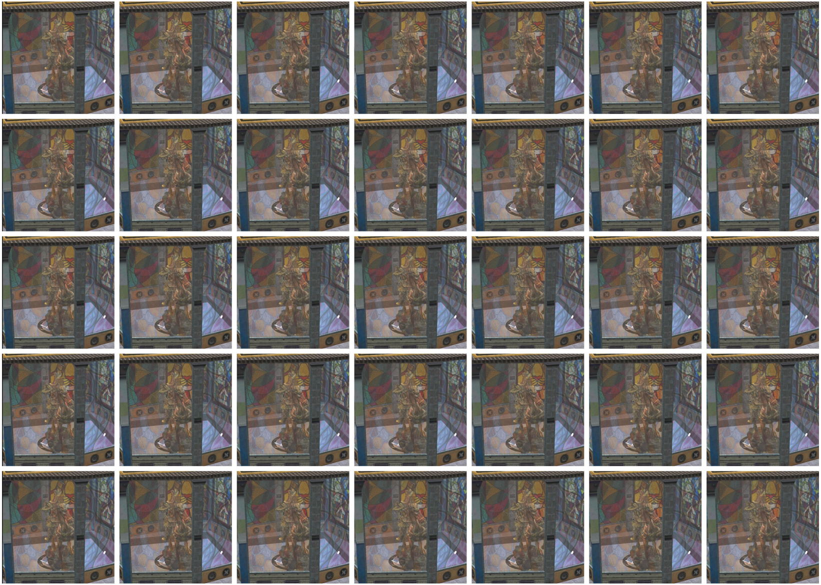

What if each of these views is actually a light field?

The light field as a dense collection of views

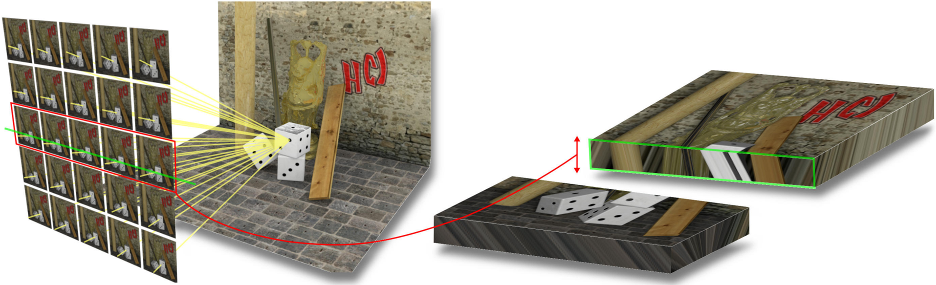

A 2D horizontal cut (green) is called an **epipolar plane image (EPI)**

[Wanner and Goldlücke, CVPR 2012 & TPAMI 2014]

Depth estimation on an epipolar plane image (EPI)

Epipolar plane image (EPI)

[Wanner and Goldlücke, CVPR 2012 & TPAMI 2014]

Depth estimation on an epipolar plane image (EPI)

Epipolar plane image (EPI)

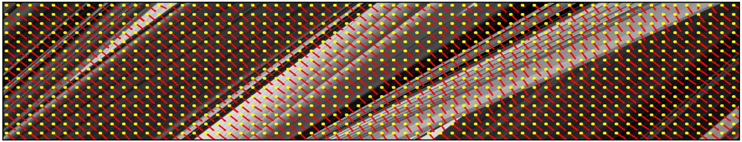

Orientation estimate (structure tensor)

[Wanner and Goldlücke, CVPR 2012 & TPAMI 2014]

Depth estimation on an epipolar plane image (EPI)

Epipolar plane image (EPI)

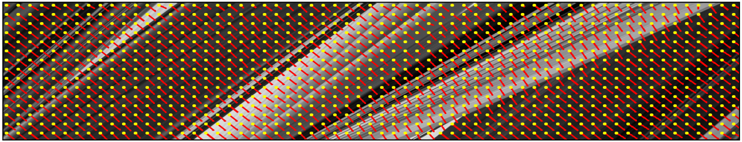

Orientation estimate (structure tensor)

Depth estimate (slope of orientation)

[Wanner and Goldlücke, CVPR 2012 & TPAMI 2014]

Dense depth via orientation estimation

light field center view

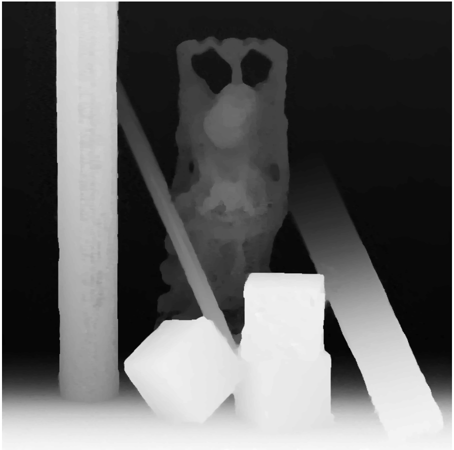

estimated depth map (denoised)

[Wanner and Goldluecke CVPR 2012, CVPR 2013, VMV 2013, TPAMI 2014]

When does depth reconstruction fail?

Unsolved: “non-cooperative” surfaces

Stereo image pair

Unsolved: "non-cooperative" surfaces

Stereo image pair

Triangulation from correspondence

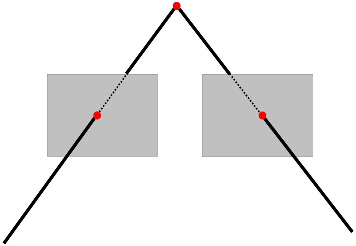

Unsolved: “non-cooperative” surfaces

Stereo image pair

Triangulation from correspondence

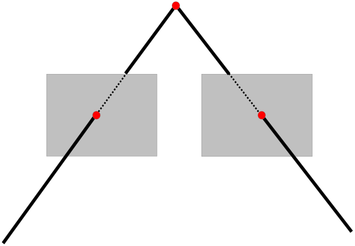

Incorrect assumption: A 3D point looks the same in all views

Unsolved: “non-cooperative” surfaces

Stereo image pair

Stereo reconstruction

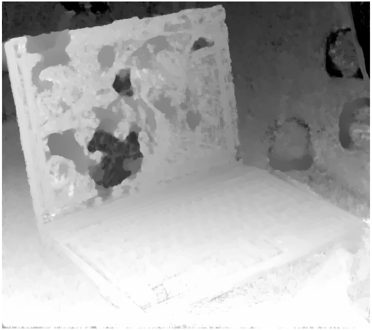

Incorrect assumption: A 3D point looks the same in all views light field

epipolar plane image closeup

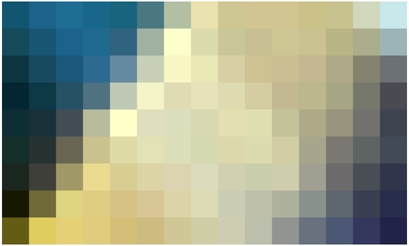

stereo reconstruction

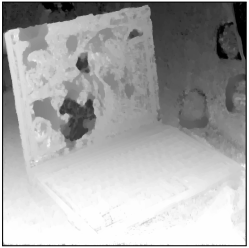

[Wanner and Goldlücke GCPR 2013]

Dealing with reflections using the light field

light field

epipolar plane image closeup

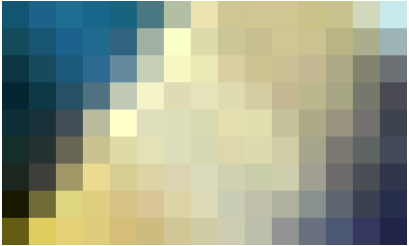

stereo reconstruction

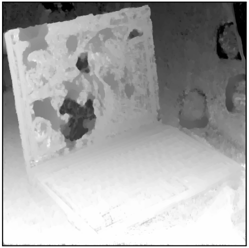

Second order structure tensor:

$$\mathcal{M} = G_\tau * \begin{bmatrix} I_{xx}^2 & I_{xx} I_{xy} & I_{xx} I_{yy} \\ I_{xy} I_{xx} & I_{xy}^2 & I_{xy} I_{yy} \\ I_{yy} I_{xx} & I_{yy} I_{xy} & I_{yy}^2 \end{bmatrix},$$

and $\boldsymbol{e}_1(\mathcal{M})$ encodes the two dominant overlaid orientations.

[Wanner and Goldlücke GCPR 2013]

Dealing with reflections using the light field

light field

epipolar plane image closeup

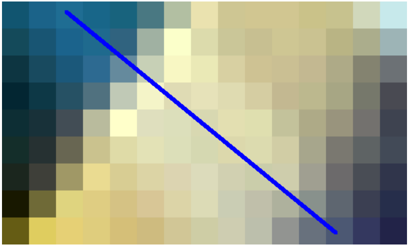

stereo reconstruction

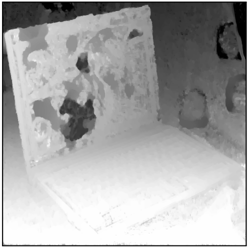

mirror plane depth

[Wanner and Goldlücke GCPR 2013]

Dealing with reflections using the light field

light field

epipolar plane image closeup

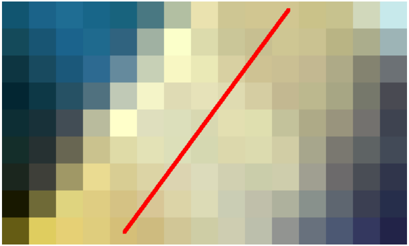

stereo reconstruction

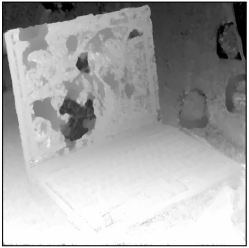

reflection depth

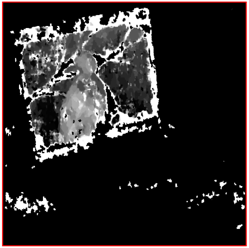

[Wanner and Goldlücke GCPR 2013]

Works great on carefully recorded data ...

light field center view

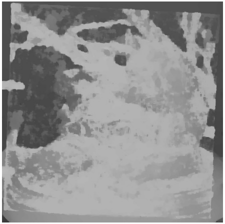

stereo reconstruction

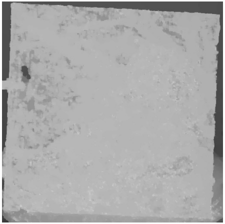

primary surface depth

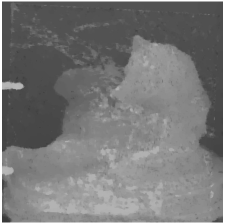

transmission depth

[Wanner and Goldlücke GCPR 2013]

Sadly, not good enough for plenoptic cameras

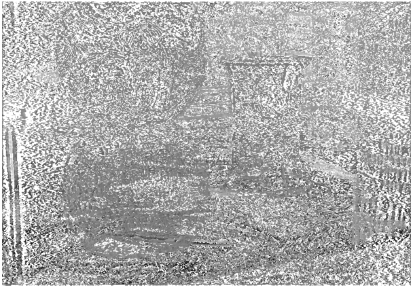

fails due to noise, too large disparity range ...

More robust layered depth reconstruction

Idea: represent each EPI patch with atoms of fixed disparity,

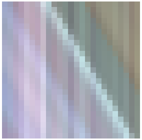

$=\ \alpha_1$

$+\ \alpha_2$

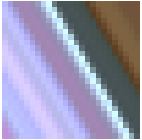

$+\ \ldots .$

Idea: represent each EPI patch with atoms of fixed disparity,

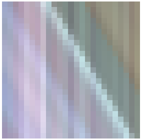 $=\ \alpha_1$  $+\ \alpha_2$ 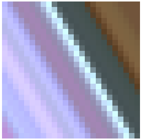 $+\ \ldots.$

Each light field patch p is assembled from a trained patch dictionary D

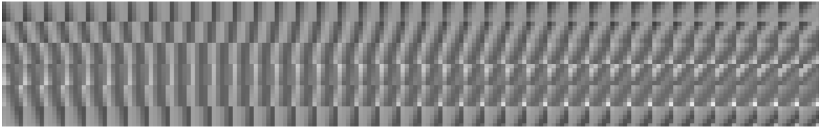

by solving the **sparse coding** problem

$$\underset{\alpha}{\operatorname{argmin}} \left\| p - D\alpha \right\|_2^2 + \lambda \left\| \alpha \right\|_1 .$$

Robust layered depth from sparse light field coding

Idea: represent each EPI patch with atoms of fixed disparity,

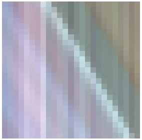 $=$ α_1  $+$ α_2 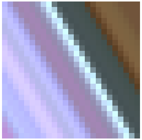 $+$ $\dots$.

Each light field patch p is assembled from a trained patch dictionary D

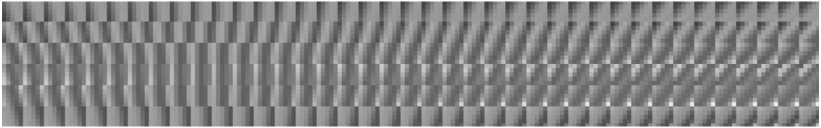

by solving the **sparse coding** problem

$$\underset{\alpha}{\operatorname{argmin}} \|p - D\alpha\|_2^2 + \lambda \|\alpha\|_1 .$$

The coding coefficients α should be related to the depth layers.

[Johannsen, Sulc, Goldluecke CVPR 2016]

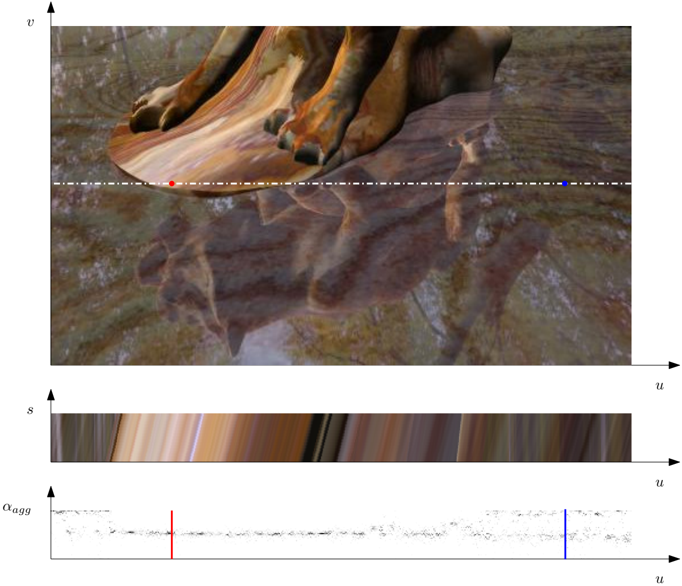
v
u
s
u
α_{agg}
u

Classes of aggregated sparse codes

- One peak - Lambertian surface
- Two peaks - Reflective/Transparent surface

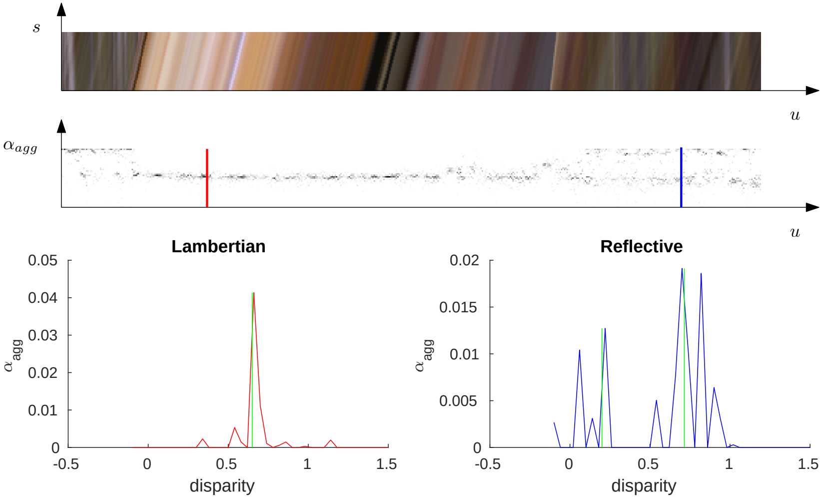

[Johannsen, Sulc, Goldluecke CVPR 2016]

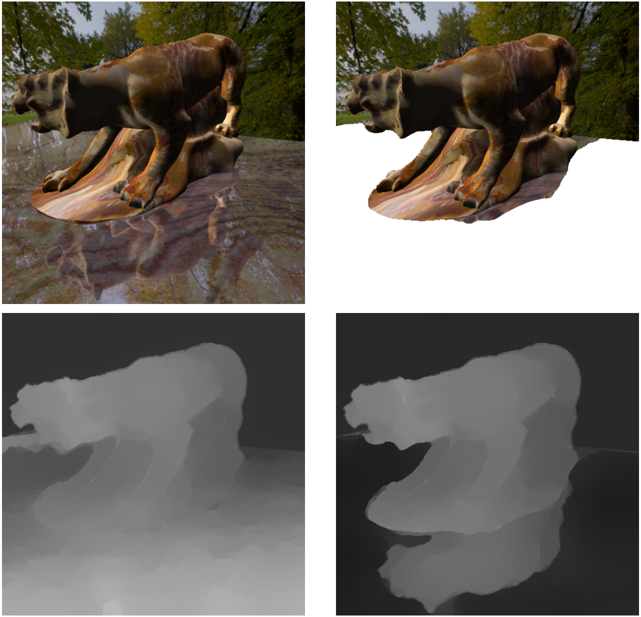

[Johannsen, Sulc, Goldluecke CVPR 2016]

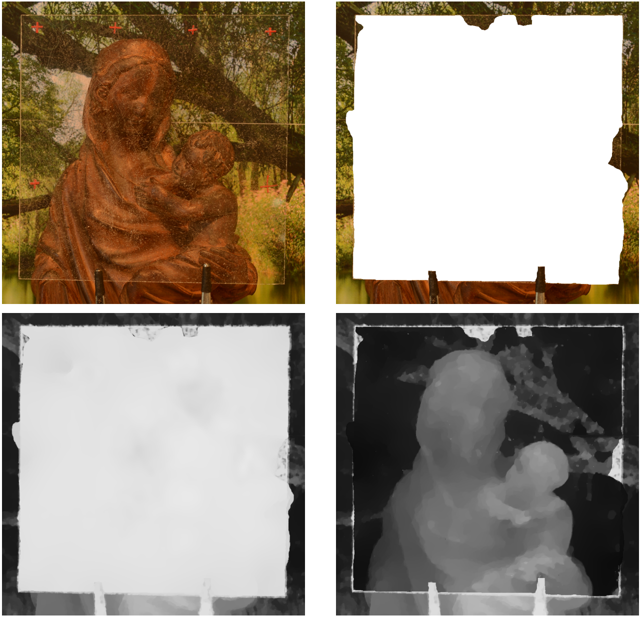

[Johannsen, Sulc, Goldluecke CVPR 2016]

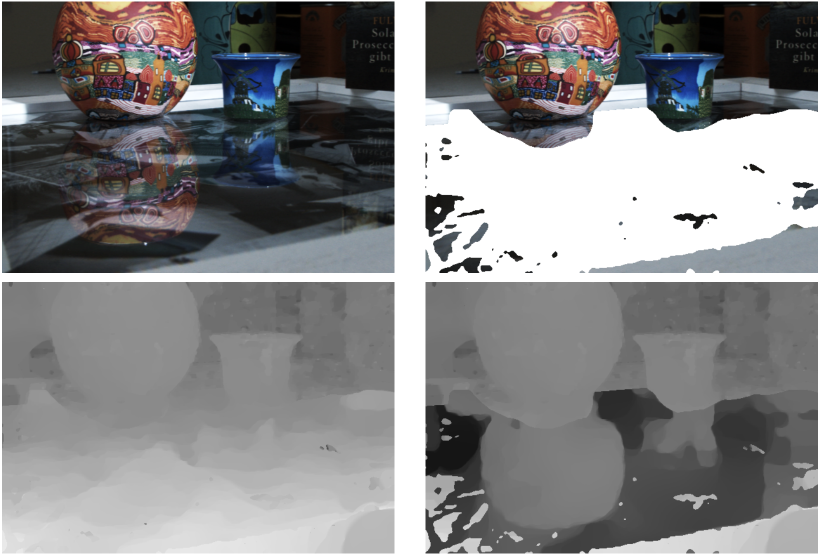

[Johannsen, Sulc, Goldluecke CVPR 2016]

Light field decomposition

[Johannsen, Sulc, Goldluecke VMV 2015]

Generative model: generates EPI from center view

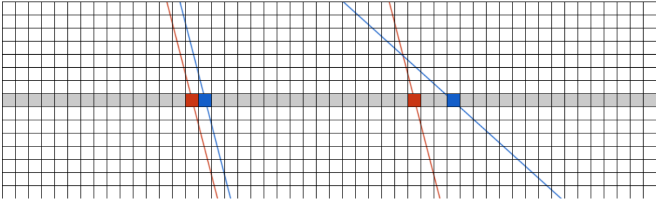

Depth-dependent linear relation between center view and EPI:

$$f = G(d_u)\, u,$$

where

u	center view image (at gray pixels),
d_u	center view depth (at gray pixels),
$G(d_u)$	depth-dependent linear transformation,
f	generated complete EPI.

[Johannsen, Sulc, Goldluecke VMV 2015]

Two-layer EPI model

Two-layer EPI synthesis **model**

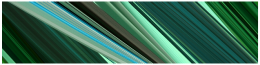 +  = 

$G(d_u)u$ $\qquad$ $G(d_v)v$ $\qquad$ f

Two-layer EPI model

Two-layer EPI synthesis **model**

$G(d_u)u$ + $G(d_v)v$ = f

Leads to **data fitting cost function**

$$D_{EPI}(u, v) = \| G_{d_u} u + G_{d_v} v - f \|_2^2$$

for each individual EPI.

[Johannsen, Sulc, Goldluecke VMV 2015]

Variational inverse problem for layer decomposition

- **Dataterm:** sum over all horizontal and vertical EPIs

$$D(u, v) = \sum_{x=1}^{W} D_x(u_x, v_x) + \sum_{y=1}^{H} D_y(u_y, v_y).$$

- **Dataterm:** sum over all horizontal and vertical EPIs

$$D\left(u,v\right) = \sum_{x=1}^{W} D_x\left(u_x,v_x\right) + \sum_{y=1}^{H} D_y\left(u_y,v_y\right).$$

- **Regularization:** total generalized variation (TGV_2), favors piecewise linear solutions

$$J(u,v) = \mathrm{TGV}_2(u) + \mathrm{TGV}_2(v).$$

- **Dataterm:** sum over all horizontal and vertical EPIs

$$D(u,v) = \sum_{x=1}^{W} D_x(u_x, v_x) + \sum_{y=1}^{H} D_y(u_y, v_y).$$

- **Regularization:** total generalized variation (TGV_2), favors piecewise linear solutions

$$J(u,v) = \mathrm{TGV}_2(u) + \mathrm{TGV}_2(v).$$

- **Total energy**:

$$E(u,v) = D(u,v) + \lambda J(u,v)$$

minimize e.g. with primal-dual method [Chambolle and Pock 2010].

[Johannsen, Sulc, Goldluecke VMV 2015]

[Johannsen, Sulc, Goldluecke VMV 2015]

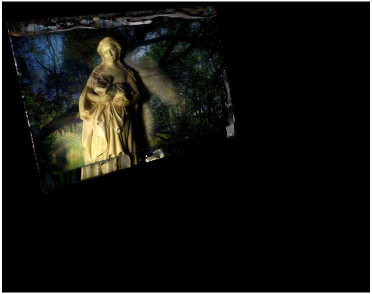

[Johannsen, Sulc, Goldluecke VMV 2015]

Outlook: intrinsic light field decomposition

Input light field (center view)

Specular component

Albedo

Shading

[Alperovich and Goldluecke, ACCV 2016]

Outlook: intrinsic light field decomposition

Input light field (center view)

Specular component

Albedo

Shading

[Alperovich and Goldluecke, ACCV 2016]

Light field camera alignment

[Johannsen, Sulc, Goldluecke ICCV 2015]

[Johannsen, Sulc, Goldluecke ICCV 2015]

Research questions

- How to estimate pose for light field cameras?
- How to easily align light fields for panoramas?
  - sparse correspondence only
  - tailored to light field geometry
  - linear algorithm

- Input: light field from pre-calibrated plenoptic camera (i.e. raw image decoded into two-plane parametrization).

Lytro camera and microlens images

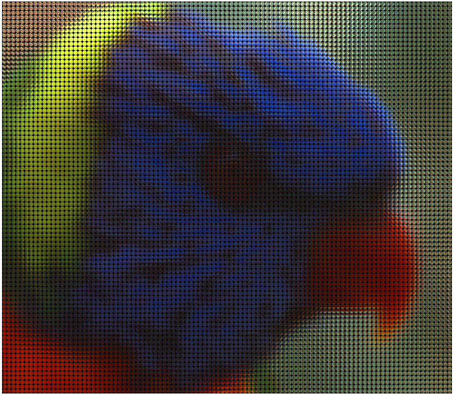


30 – 250mm f/2
LIGHT FIELD OPTICS

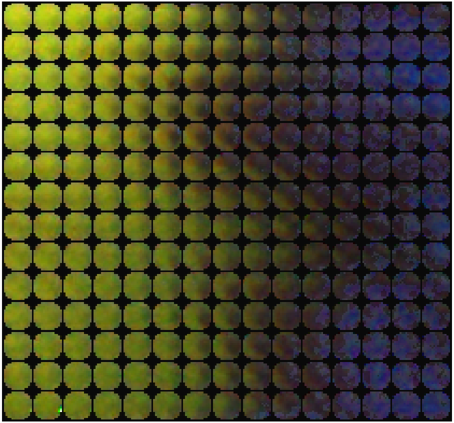

How to get to array of views (subaperture images)?

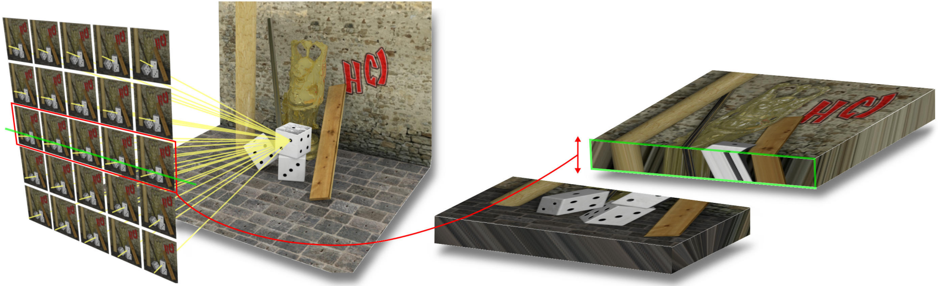

Illustration by Sven Wanner

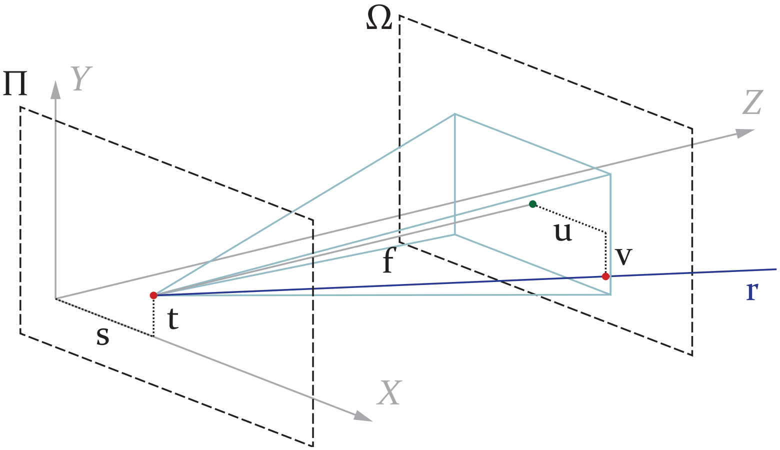
Ω
Π
Y
Z
u
v
f
r
t
s
X

What is the projection of a 3D point $\boldsymbol{X}$ into a light field?

What is the projection of a 3D point $\boldsymbol{X}$ into a light field?

A 2D subspace in the 4D ray space, which can be parametrized in 5D homogenous light field coordinates as follows:

$$\underbrace{\begin{bmatrix} 1 & 0 & \frac{f}{Z} & 0 & -\frac{fX}{Z} \\ 0 & 1 & 0 & \frac{f}{Z} & -\frac{fY}{Z} \end{bmatrix}}_{=:M(\boldsymbol{X},f)} \begin{bmatrix} u \\ v \\ s \\ t \\ 1 \end{bmatrix} = 0.$$

Note: these are just the projection equations of a pinhole camera located in (s, t).

What are correspondences between two light fields?

What are correspondences between two light fields?

- Ideally, correspondences between subspaces (todo).

What are correspondences between two light fields?

- Ideally, correspondences between subspaces (todo).
- In practice, matched features between subaperture images:

$$\{\boldsymbol{l}_i\}_{i=1,\dots n} \leftrightarrow \{\boldsymbol{l}'_j\}_{j=1,\dots,m}.$$

where $\boldsymbol{l}, \boldsymbol{l}'$ are 4D light field coordinates in two different light fields - i.e. rays.

What are correspondences between two light fields?

- Ideally, correspondences between subspaces (todo).
- In practice, matched features between subaperture images:

$$\{\boldsymbol{l}_i\}_{i=1,\dots n} \leftrightarrow \{\boldsymbol{l}'_j\}_{j=1,\dots,m}.$$

  where $\boldsymbol{l}, \boldsymbol{l}'$ are 4D light field coordinates in two different light fields - i.e. rays.

- obtained e.g. from matching SIFT features across all subaperture images, absurd matches pre-eliminated (if e.g. disparity outside a sensible range).

- **Obvious observation**: a single LF correspondence leads to two corresponding 3D points.

- **Obvious observation**: a single LF correspondence leads to two corresponding 3D points.

- Trivial strategy for pose estimation: compute 3D points for all LHS and RHS of a correspondence, align two corresponding 3D point clouds.

- **Obvious observation**: a single LF correspondence leads to two corresponding 3D points.
- Trivial strategy for pose estimation: compute 3D points for all LHS and RHS of a correspondence, align two corresponding 3D point clouds.
- Turns out this is both boring as well as bad.

Light field camera pose: strategy II

Blackboard time: Plücker ray coordinates and GEC

Blackboard time: Plücker ray coordinates and GEC

- Generalized epipolar constraint:

$$\boldsymbol{q}'^{\,T} E \boldsymbol{q} + \boldsymbol{q}'^{\,T} R \boldsymbol{m} + \boldsymbol{m}'^{\,T} R \boldsymbol{q} = 0.$$

where $E = [t]_\times R$ is the essential matrix, and the camera coordinate systems are related by a rotation R and translation t according to

$$\boldsymbol{X}' = R\boldsymbol{X} + t.$$

- Note number of equations: $n \cdot m$ per correspondence.

Linear correspondence constraints in light fields?

Linear correspondence constraints in light fields?

Observation I: projection from Plücker ray coordinates into homogenous light field coordinates is projective-linear:

$$q_3' \begin{bmatrix} u' \\ v' \\ s' \\ t' \\ 1 \end{bmatrix} = \begin{bmatrix} f & 0 & 0 & 0 & 0 & 0 \\ 0 & f & 0 & 0 & 0 & 0 \\ 0 & 0 & 0 & 0 & -1 & 0 \\ 0 & 0 & 0 & 1 & 0 & 0 \\ 0 & 0 & 1 & 0 & 0 & 0 \end{bmatrix} \begin{bmatrix} R & 0 \\ E & R \end{bmatrix} \begin{bmatrix} q \\ m \end{bmatrix}.$$

Observation II: Each ray in a correspondence must lie in the subspace of the correspondence when transformed into the respective other light field.

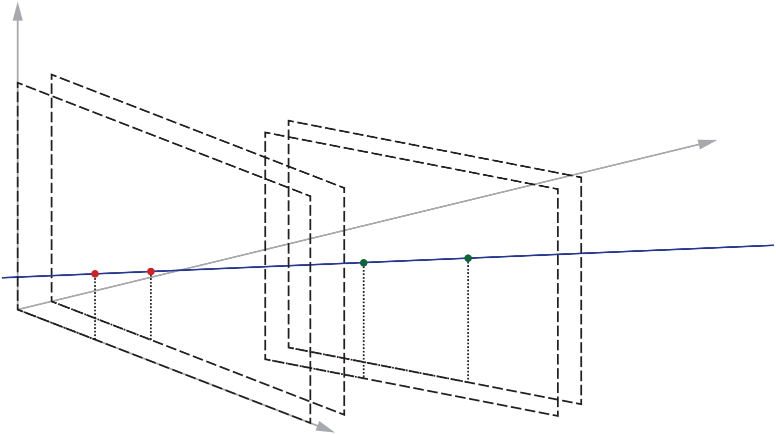

Given a correspondence

$$\{\boldsymbol{l}_i\}_{i=1,\dots n} \leftrightarrow \{\boldsymbol{l}'_j\}_{j=1,\dots,m}$$

estimate subspace matrices M and M' for LHS and RHS.

Given a correspondence

$$\{\boldsymbol{l}_i\}_{i=1,\dots n} \leftrightarrow \{\boldsymbol{l}'_j\}_{j=1,\dots,m}$$

estimate subspace matrices M and M' for LHS and RHS.

Each ray on the LHS must satisfy

$$M' P(f) \begin{bmatrix} R & 0 \\ E & R \end{bmatrix} \begin{bmatrix} \boldsymbol{q} \\ \boldsymbol{m} \end{bmatrix} = 0.$$

Light field camera pose: proposed strategy

Given a correspondence

$$\{\boldsymbol{l}_i\}_{i=1,\dots n} \leftrightarrow \{\boldsymbol{l}'_j\}_{j=1,\dots,m}$$

estimate subspace matrices M and M' for LHS and RHS.

Each ray on the LHS must satisfy

$$M' P(f) \begin{bmatrix} R & 0 \\ E & R \end{bmatrix} \begin{bmatrix} \boldsymbol{q} \\ \boldsymbol{m} \end{bmatrix} = 0.$$

Abbreviate with M_1 the first three and with M_2 the second three columns of the 2×6 matrix $M' P(f)$,

$$M_1 R \boldsymbol{q} + M_2 R \boldsymbol{m} + M_1 E \boldsymbol{q} = 0.$$

Same form as GEC, same algorithm to compute solution.
Note: only $2(n+m)$ equations per correspondence instead of $n \cdot m$.

Can be re-arranged to

$$A_E \mathrm{vec}(E) + A_R \mathrm{vec}(R) \ = \ 0.$$

with matrices E, R stacked to columns $\mathrm{vec}(E), \mathrm{vec}(R)$.

Can be re-arranged to

$$A_E \mathrm{vec}(E) + A_R \mathrm{vec}(R) \ = \ 0.$$

with matrices E, R stacked to columns $\mathrm{vec}(E), \mathrm{vec}(R)$.

Solution for $\mathrm{vec}(R)$ s.t. $\|\mathrm{vec}(R)\| = 1$ satisfies

$$(A_E A_E^+ - I) A_R \mathrm{vec}(R) = \mathbf{0}.$$

Solve using SVD, project to $SO(3)$ to obtain linear estimate for R.

Can be re-arranged to

$$A_E \mathrm{vec}(E) + A_R \mathrm{vec}(R) \ = \ 0.$$

with matrices E, R stacked to columns $\mathrm{vec}(E), \mathrm{vec}(R)$.

Solution for $\mathrm{vec}(R)$ s.t. $\|\mathrm{vec}(R)\| = 1$ satisfies

$$(A_E A_E^+ - I) A_R \mathrm{vec}(R) = \mathbf{0}.$$

Solve using SVD, project to $SO(3)$ to obtain linear estimate for R.

Linear estimate for t follows from substituting solution for R into above equation.

Non-linear refinement

In theory, solution is subject to difficult non-linear constraints:

- R must be a rotation,
- $E = [t]_\times R$,

so it is not expected that the linear estimate is sufficient.

In theory, solution is subject to difficult non-linear constraints:

- R must be a rotation,
- $E = [t]_\times R$,

so it is not expected that the linear estimate is sufficient.

Previous work: “iterative refinement”, solve for R and t in turn, backproject to allowed space of solutions.

Non-linear refinement

In theory, solution is subject to difficult non-linear constraints:

- R must be a rotation,
- $E = [t]_\times R$,

so it is not expected that the linear estimate is sufficient.

Previous work: “iterative refinement”, solve for R and t in turn, backproject to allowed space of solutions.

In practice, not necessary **if solving for R first instead of E.**

Focal length

Can be done by brute force search, just look for f which minimizes residual in the linear system - not elegant, but works. Full non-linear bundle adjustment as a second step of course possible as well.

Light field camera pose: comparison

	Correspondences	10 matches, 10 projections per point					20 matches, 10 projections per point					10 matches, 20 projections per point				
	Noise level σ_{uv}	0.2	0.4	0.6	0.8	1.0	0.2	0.4	0.6	0.8	1.0	0.2	0.4	0.6	0.8	1.0
Angular rot. error [deg]	*linear methods*															
	3DPC	1.82	5.19	8.93	11.56	16.18	1.33	3.42	6.77	8.38	10.24	1.15	4.35	6.43	9.14	14.12
	R2R-O	2.04	11.17	15.37	37.48	43.32	0.72	2.19	3.48	3.76	6.41	1.87	3.01	17.56	39.66	40.02
	R2R-I	0.88	1.91	3.51	4.55	5.19	0.40	0.92	2.13	2.76	4.01	0.55	1.40	2.64	4.20	5.98
	Proposed	**0.65**	**1.19**	1.80	2.28	3.15	0.27	0.52	0.83	1.11	1.49	0.40	0.81	1.27	1.77	**2.39**
	with refinement															
	R2R-O-R20	1.00	2.05	3.71	4.53	18.40	0.43	0.90	2.31	2.94	4.10	0.62	1.45	9.27	7.86	9.33
	R2R-I-R20	1.00	2.18	3.83	4.73	5.21	0.43	0.91	2.32	2.95	4.11	0.64	1.50	2.74	4.45	6.08
	Proposed-R20	0.69	1.20	**1.77**	**2.23**	**2.85**	**0.26**	**0.50**	**0.79**	**1.05**	**1.42**	**0.37**	**0.80**	**1.18**	**1.57**	2.39
Relative transl. error [%]	*linear methods*															
	3DPC	0.28	0.82	0.93	2.19	2.20	0.32	0.97	0.92	1.44	0.95	0.46	0.84	1.21	0.74	0.86
	R2R-O	0.20	1.15	1.06	4.18	2.01	0.05	0.43	0.30	0.36	0.45	1.68	0.27	1.43	0.98	0.79
	R2R-I	0.04	0.12	0.23	0.46	0.52	0.02	0.09	0.14	0.25	0.36	0.12	0.11	0.27	0.24	0.33
	Proposed	**0.03**	**0.07**	0.15	**0.25**	0.24	**0.01**	0.05	**0.07**	**0.11**	0.14	0.13	**0.06**	0.16	0.10	**0.12**
	with refinement															
	R2R-O-R20	0.05	0.13	0.24	0.51	0.67	0.02	0.09	0.15	0.25	0.36	0.12	0.11	0.41	0.27	0.37
	R2R-I-R20	0.04	0.13	0.24	0.51	0.51	0.02	0.09	0.15	0.25	0.36	0.12	0.11	0.27	0.25	0.33
	Proposed-R20	0.03	0.08	**0.14**	0.26	**0.23**	0.01	**0.05**	0.07	0.11	**0.14**	**0.11**	0.06	**0.16**	**0.10**	0.13

Accuracy of the different methods both before and after non-linear refinement. Different numbers of correspondences N, projections per correspondence K, and levels of noise σ_{uv} on the (u, v)-coordinates are compared. Error metrics are the angular deviation from the ground truth in degrees for the estimated rotation, as well as the relative translation error measured as a percentage of the length of the ground truth translation vector. Noise standard deviation is given in units of pixels on the subaperture images. In all cases, the most accurate method (highlighted in bold) is the one proposed in this paper.

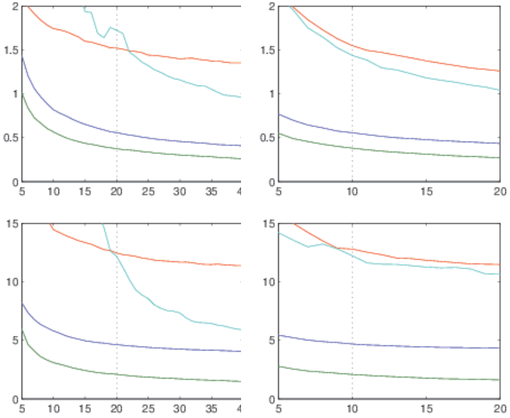

The graphs show how the angular error in rotation depends on the number of matches (left) and the number of rays per match (right). Compared are the four linear methods in table **??**: 3DPC [**?**] (red) and R2R-O [**?**] (cyan), R2R-I with our proposed numerical improvements (blue), and finally the novel proposed method for 4D light fields (green). Top row: small amount of noise ($\sigma = 0.2$), bottom: large amount of noise ($\sigma = 1.0$).

Living panoramas

3D point cloud

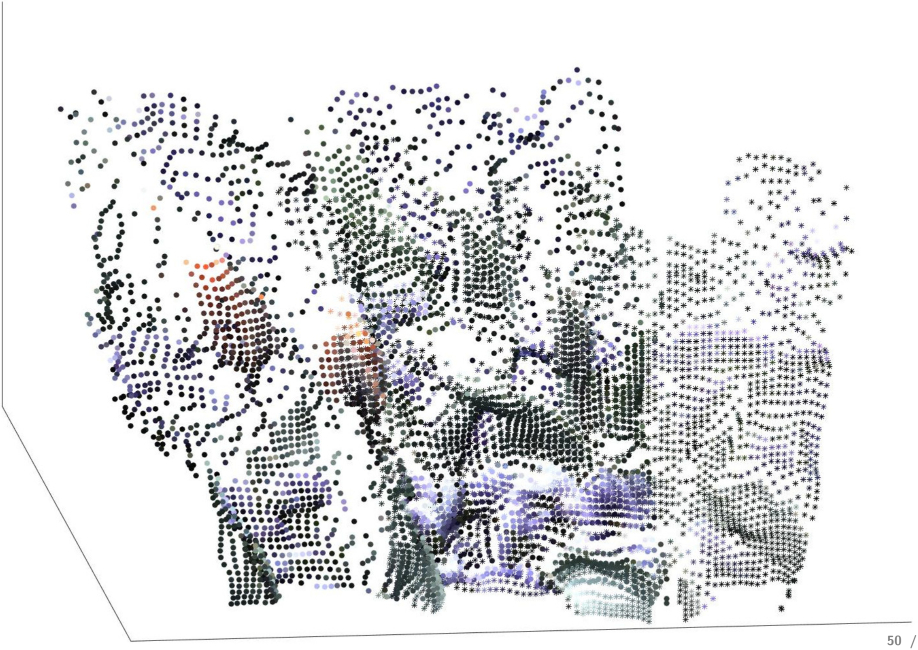

Conclusions

- Simple linear method to estimate pose for light fields in the two-plane parametrization.
- More accurate than all previous methods, reduced number of equations compared to framework of generalized cameras.
- Allows simple construction of refocusable light field panoramas, but there's work left to do for high quality.

Putting it all together - full scene reconstruction

Let's go back to our challenge dataset

Light field alignment and bundle adjustment

Two-layered depth map estimation

Center view 14 / 24

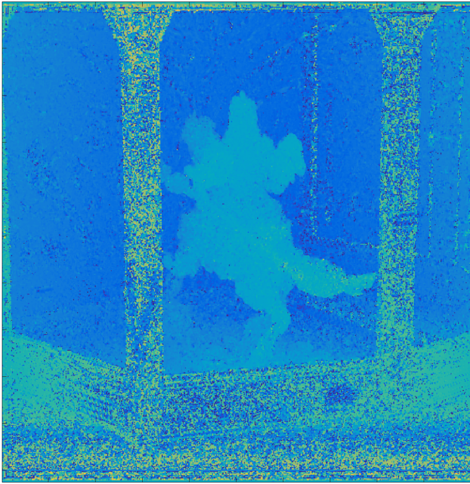

Depth second layer

Input

reconstruction

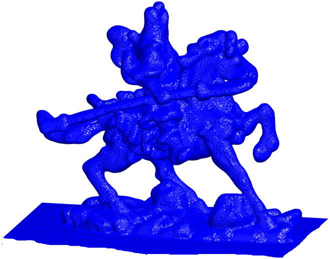

ground truth

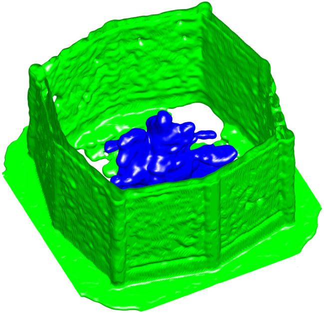

Summary

Sparse light field coding for multi-layer depth
[Johannsen, Sulc, Goldluecke CVPR 2016, GCPR 2016]

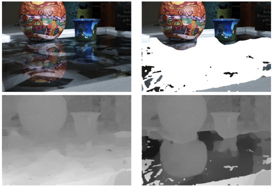

Light field decomposition and intrinsic light fields
[Johannsen, Sulc, Goldluecke VMV 2015,
Alperovich and Goldluecke (submitted to ACCV 2016)]

Light field alignment and refocusable panoramas
[Johannsen, Sulc, Goldluecke ICCV 2015]

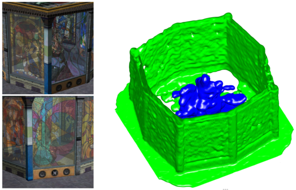

Multi-layered 3D scene reconstruction
[Johannsen, Sulc, Marniok, Goldluecke (submitted)]